

**Degrees of freedom and the phase transitions of two-flavor QCD**Topi Kähärä\* and Kimmo Tuominen<sup>+</sup>*Department of Physics, University of Jyväskylä, Finland  
Helsinki Institute of Physics, University of Helsinki, Finland  
(Received 10 April 2008; published 15 August 2008)*

We study two effective models for QCD, the Nambu-Jona-Lasinio -model and the linear sigma model extended by including a Polyakov loop potential, which is fitted to reproduce the pure gauge theory thermodynamics, and a coupling between the chiral fields and the Polyakov loop. Thus the resulting models have as relevant degrees of freedom the Polyakov loop and chiral fields. By comparing the extended models with the bare chiral models we can conclude that the addition of the Polyakov loop is necessary in order to obtain both qualitative and quantitative agreement with known results at finite temperatures. These results are extended to finite net-quark densities, several thermodynamical quantities are investigated in detail, and possible applications and consequences for relativistic heavy ion collision phenomenology are discussed.

DOI: [10.1103/PhysRevD.78.034015](https://doi.org/10.1103/PhysRevD.78.034015)

PACS numbers: 12.38.Aw, 12.38.Mh

**I. INTRODUCTION**

Phase transitions in strongly interacting matter have been a subject of intense theoretical, computational and experimental research over the past decades. Apart from the values of quark masses and numbers of colors and flavors relevant for the physical QCD, a lot of effort has been devoted to understand different limits of the theory as these parameter values are varied. Several qualitative and in some cases quantitative aspects have been revealed; for example, we know that in the absence of quarks the  $SU(N)$  Yang-Mills theory has a global  $Z_N$  symmetry [1], and there exists a gauge-invariant operator charged under  $Z_N$ , the Polyakov loop, which can be identified as the order parameter of the theory. Hence, the deconfinement phase transition can be characterized using the universality arguments [2]. Numerical studies have confirmed this picture as it has been found that the deconfinement phase transition is second order when the number of colors is  $N_c = 2$  [3], first order for  $N_c = 3$  [4] (although weakly [5]), and presumably first order for  $N_c \geq 4$  [6].

Adding quarks to the theory changes the picture considerably. For light fermions in the fundamental and pseudoreal representations for  $N_c = 3$  and  $N_c = 2$ , respectively, the corresponding  $Z_3$  or  $Z_2$  the center of the gauge group is not anymore a good symmetry. However, the exact chiral symmetry of massless fermions is only little perturbed by small masses and the order parameter is the chiral condensate which characterizes the chiral phase transition. For  $N_c = 3$  and two massless quark flavors at finite temperature and zero net baryon density, the chiral phase transition is in the same universality class as the three dimensional  $O(4)$  spin model [7], becoming a smooth crossover as

small quark masses are accounted for [8]. For  $N_c = 2$  the relevant universality class is that of  $O(6)$  [9].

In addition to finite temperature, one can also study the response of the QCD vacuum by considering finite net quark densities. At finite chemical potential one needs to take into account the pairing phenomena and superconducting phases result. However, a systematic approach based on the full QCD dynamics can be applied only in asymptotically high densities [10] where asymptotic freedom simplifies the analysis. To determine the phases at intermediate densities relevant for phenomenological applications one needs to resort to effective models. Within the model studies taking into account the patterns of chiral symmetry breaking, one usually hopes to gain insight on the qualitative aspects of the phase diagram. Studies within different models have revealed that in cold dense matter, a first order phase transition to a superconducting phase characterized by nonzero diquark condensate takes place. Contrasting this with the finite temperature crossover transition at  $\mu = 0$  one concludes that in the  $(T, \mu)$ -plane there must exist a critical endpoint. A central paradigm for the first-principle studies of the QCD equation of state [11] in the  $(T, \mu)$ -plane is therefore the existence and location of this critical point as well as its other properties. The lattice determinations using different techniques have provided estimates for the location of the critical point. For two flavors see [12,13]. The existence of the critical point in three flavor QCD is currently under debate, [14,15], and in any case one should be careful in drawing any conclusions from the  $N_f = 2$  results to the physical  $N_f = 2 + 1$  case.

The perturbative calculations for cold quark matter at asymptotically large chemical potential or for hot quark gluon gas at high temperature cannot be directly applied to the phenomenologically relevant densities and temperatures. At finite temperature the perturbation expansion is known to converge poorly and reliable results can be obtained only at near-zero chemical potential well above

\*topi.kahara@phys.jyu.fi

<sup>+</sup>kimmo.tuominen@phys.jyu.fi

the suitably defined transition temperature  $T \geq 3T_c$ , where the picture of weakly interacting dressed quark and gluon quasiparticles obviously becomes correct. To address quantitative phenomenology for all temperatures at zero net quark density, a numerical “recipe” for interpolating smoothly between thermodynamics described by perturbation theory at high temperatures and by a resonance gas at low temperatures was proposed in [16], taking also into account the contribution of quarks with finite masses. This approach provides one with a working definition of  $p(T, \{m_i\})$ ,  $i = 1, \dots, N_f$  and of the resulting thermodynamics, but it does not yield insight to the nature of the underlying effective degrees of freedom and mechanisms responsible for the dynamics between the thermally dressed hot quarks and gluons and low temperature hadronic resonances. Lattice results at finite baryochemical potential have been compared with hadron resonance gas calculations e.g. in [17].

In this work we concentrate on the case of QCD with two light quark flavors and study a particular effective model description of it. This effective model is based on the following picture: As a function of the quark mass there exist two separate dynamical sectors. For massless quarks there is spontaneous breaking of exact chiral symmetry, while if the quarks are very heavy, and decouple from the dynamics, the center symmetry and its spontaneous breaking becomes relevant. In real QCD neither of these two is exact. Lattice calculations indicate that for quarks with finite masses, the transition is a smooth crossover as is also expected on the basis of universality arguments, and the transition can be located by measuring the expectation value of the chiral condensate. However, even if the discrete symmetry associated with deconfinement is broken by the presence of light quarks, one can still study the temperature dependence of the Polyakov loop on the lattice. This has been done, and one observes the Polyakov loop to rise from zero to one as temperature is increased from low to high values. Because of this behavior one also speaks of deconfining phase transition [18]. Moreover, the lattice results [18] indicate that at zero chemical potential chiral symmetry breaking and confinement (i.e. a decrease of the Polyakov loop) occur at the same critical temperature. Several attempts to explain these behaviors exist [19]. Relying only on the exact and approximate symmetries of the system and general effective field theory methods a qualitative solution to this puzzle was established in [20] based on the idea of transfer of information from the order parameters to noncritical fields. As a function of quark mass, from light to heavy quarks, this mechanism allows one to treat either chiral symmetry or center symmetry as the relevant one driving the transition and through interactions allowing also the other would-be-order parameter field to behave in a similar way. The framework proposed in [20] also explains the independence of deconfinement and chiral symmetry restoration in the case of adjoint

quarks which do not break the center symmetry. The  $(T, \mu)$  phase diagram for adjoint two color QCD was considered in detail in [21].

This behavior has been reanalyzed and confirmed in numerical studies of the NJL model and linear sigma model coupled to the Polyakov loop via quarks which are integrated out in the random phase approximation [22–25]. In this work we study the coupling of Polyakov loop and chiral degrees of freedom described either with the linear sigma model (LSM) or the Nambu-Jona-Lasinio (NJL) model, and compare the resulting thermodynamics to that of two-flavor QCD. Inclusion of the Polyakov loop makes the result qualitatively and, to some extent, even quantitatively insensitive to the underlying model which is used to describe the chiral degrees of freedom at finite temperature and small values of quark chemical potential. The importance of the Polyakov loop is not surprising, since the gluonic degrees of freedom are known to be important for the bulk thermodynamics of QCD matter when the net baryon densities are small. We consider also finite densities, and show that quantitative discrepancy between the two models increases as larger values of chemical potential are considered. To display this concretely, we determine the location of the critical point in the  $(T, \mu)$ -plane and show how the two models lead to very different results.

The effective models studied here may provide input to the phenomenology of relativistic heavy ion collisions. Recently, with the advent of RHIC data, it has been established that the spacetime evolution of the hot dense QCD matter is well described by nearly ideal hydrodynamics. This means, in particular, that the system evolves along the lines of constant  $S/N$ . Hence, we study, in particular, the behavior of isentropic lines in the  $(T, \mu)$  phase diagram in these two models. Whether these have the tendency to focus on the critical point is important for the possible experimental discovery of the critical point in heavy ion collisions. We find that in these models such strong focusing behavior does not exist.

We introduce the models in some detail in Sec. II, and carry out an analysis of the thermodynamics in Sec. III. Comparing these models at zero chemical potential, we find that they imply very similar results. We also compare with the results of the resummed perturbation theory [16]. At finite chemical potential we find that the quantitative results of the models show large deviations. Especially the location of the QCD critical point cannot be estimated reliably within these models. We end with concluding remarks and discussion of further prospects in Sec. IV.

## II. MODELS

The chiral dynamics of two-flavor QCD is often formulated in terms of a linear or nonlinear sigma model, which treats the Goldstone bosons as the relevant degrees of freedom. Of these two possibilities, the linear representa-

tion is more useful to study the finite temperatures and densities in order to find the phase diagrams of the theory, since also the order parameter is included explicitly. Yet another possibility is to treat the fundamental fermion fields as basic degrees of freedom, the mesons appearing as the bound states of the theory, and this leads to NJL models. The effects of small quark masses are taken into account in the effective model Lagrangians by terms explicitly breaking chiral symmetry. These terms, appearing with small coefficients, render the chiral symmetry of the theory only approximate. Both of the above mentioned effective models for the phenomenology of two-flavor QCD can be parametrized to describe equally well the vacuum structure at  $T = \mu = 0$ .

Finite temperature dynamics of  $SU(N)$  pure gauge theory on the other hand is represented by  $Z_N$  symmetric effective theory for which the order parameter is the Polyakov loop. Polyakov loop can be constructed and studied also in a theory with quarks even though the presence of fermions in the fundamental representation of the gauge group breaks the center symmetry explicitly due to the antiperiodic boundary conditions of the fermion fields at finite temperature.

Therefore, in real QCD neither chiral symmetry or the center symmetry is exact, and we know that the finite temperature phase transition at  $\mu = 0$  is a smooth crossover. However, one may ask which of the two symmetries is more accurate and would act as a “driving force” for the transition. Since chiral symmetry breaking is proportional to  $m_q$ , and  $Z_N$  breaking is proportional to  $1/m_q$ , in the case of two light flavors, it seems natural to consider the system to have an approximate chiral symmetry. This expectation is strengthened also by looking at the spectrum of the bound states, as the pions clearly show the approximate Goldstone behavior. Based on these motivations, in [20] the situation was considered taking the  $m_q = 0$  limit in which the chiral symmetry becomes exact, while the  $Z_N$  symmetry is completely broken. Then the general principles of effective theory dictate the following form for the potential

$$\mathcal{L}[\sigma, \pi^a, \phi] = \mathcal{L}_0[\sigma, \pi^a] + \mathcal{L}_0[\phi] + \mathcal{L}_{\text{int}}[\sigma, \pi^a, \phi], \quad (1)$$

where  $\mathcal{L}_0[\sigma, \pi^a]$  is the chiral Lagrangian which has exact chiral symmetry,  $\mathcal{L}_0[\phi]$  is the potential for the Polyakov loop and contains both  $Z_N$  symmetric and symmetry violating terms and finally  $\mathcal{L}_{\text{int}}$  is the part containing the interactions between the chiral fields and the Polyakov loop. As shown in [20], the most important term for the dynamics is  $\sim \phi(\sigma^2 + \pi^2)$ , which leads to transfer of information between the order parameter and a nonorder parameter field. When quark mass is increased away from the chiral limit, the transition becomes a smooth crossover, but the coincidence of the chiral symmetry restoration and

deconfinement is expected as long as chiral symmetry remains good approximation.

On the other hand one can consider infinitely heavy quarks, i.e. the pure gauge limit. Then the mechanism described above works similarly, but the roles of chiral symmetry and center symmetry are switched and the deconfinement order parameter drives the change of the chiral condensate. Again the two phenomena will coincide. Decreasing the quark mass from the pure gauge limit, the first order deconfinement line is expected to terminate at a critical point at some value of quark mass and for smaller values become a smooth crossover. Since lattice investigations find coincidence of critical temperatures related to chiral symmetry restoration and deconfinement for the accessible quark masses, it is reasonable to expect that in the  $(m_q, T)$  plane there is a single phase border interpolating between these well-known small and large quark mass behaviors. The results of [20] can be applied to understand the behaviors near either small or large quark mass critical points. For intermediate values, more specific model studies or first principle lattice calculations are needed.

A specific model framework claimed applicable for all values of  $m_q$  was proposed in [22,23]. In the present work we study this framework in detail. We consider, side-by-side, both the NJL model and the linear sigma model (LSM) for two mass-degenerate quark flavors coupled to the Polyakov loop. The important feature underlying the dynamics in the approaches [22,23,25] is the assumption of independent deconfinement and chiral symmetry restoration described by the order parameters  $\phi$  and  $\sigma$ , respectively, and having independent effective potentials,  $U_\phi$  and  $U_\sigma$ , connected by interactions between the two. The central further assumption, then, is that the proposed interaction term yields the correct form for the resulting effective potential at all values of the quark mass, i.e. interpolates correctly between the limits of exact center symmetry and exact chiral symmetry hence describing also correctly the behaviors at the point  $(m_{\text{phys}}, T)$ , corresponding to the real two-flavor QCD. We aim to test this underlying assumption in detail by cartographing the thermodynamics of these models over the  $(T, \mu)$  plane and study in quantitative detail these two models against each other as well as against the numerical knowledge of real two-flavor QCD at zero net quark density. Let us start by describing the details of the models we use. To derive the grand canonical potential, we consider the following Lagrangian

$$\mathcal{L} = \mathcal{L}_{\text{chiral}} + U_\phi, \quad (2)$$

where we have separated the contributions of chiral degrees of freedom and the Polyakov loop. The part  $\mathcal{L}_{\text{chiral}}$  is for the LSM and NJL models, respectively,

$$\begin{aligned} \mathcal{L}_{\text{chiral}} = & \bar{q}(i\gamma^\mu(\partial_\mu - ig_s A_0 \delta_{\mu 0}) - g(\sigma + i\gamma_5 \vec{\tau} \cdot \vec{\pi}))q \\ & - \frac{\lambda^2}{4}(\sigma^2 + \pi^2 - v^2)^2 + H\sigma, \quad \text{LSM} \end{aligned} \quad (3)$$

$$\mathcal{L}_{\text{chiral}} = \bar{q}(i\gamma^\mu(\partial_\mu - ig_s A_0 \delta_{\mu 0}) - m_0)q - \frac{(M - m_0)^2}{2G}, \quad \text{NJL} \quad (4)$$

where  $q = (u, d)$  is the light quark field,  $m_0$  the bare quark mass ( $m_0 = m_u = m_d$ , i.e. exact isospin is assumed),  $\sigma$  and  $\vec{\pi}^T = (\pi^1, \pi^2, \pi^3)$  constitute a chiral field  $\Sigma^T = (\sigma, \vec{\pi})$  and finally  $M = m_0 - G\langle\bar{q}q\rangle$ . We work under the mean field approximation, hence the kinetic term of the chiral field is neglected in (3) and the four-fermion interaction of the NJL-model Lagrangian has been linearized in the condensate  $\langle\bar{q}q\rangle$  in (4). The symmetry breaking field  $H$  in (3) is  $H = f_\pi m_\pi^2$ , where  $f_\pi = 0.093$  GeV and  $m_\pi = 0.138$  GeV. The coupling  $\lambda^2$  is determined by the tree level mass  $m_\sigma^2 = 2\lambda^2 f_\pi^2 + m_\pi^2$ , which is set to be 0.60 GeV. In vacuum the expectation values of the fields are  $\sigma = f_\pi$  and  $\pi = 0$ . Requiring that the constituent mass in vacuum is about 1/3 of the nucleon mass yields  $g = 3.3$ . In the NJL model the bare quark mass  $m_0$  is taken to be 5.5 MeV and the coupling  $G = 10.08$  GeV<sup>-2</sup>. For a summary of the parameter values see Table I.

The Polyakov loop is included through the mean field potential

$$U(\phi, \phi^*, T)/T^4 = -\frac{b_2(T)}{2}|\phi|^2 - \frac{b_3}{6}(\phi^3 + \phi^{*3}) + \frac{b_4}{4}(|\phi|^2)^2, \quad (5)$$

where

$$b_2(T) = a_0 + a_1 \frac{T_0}{T} + a_2 \left(\frac{T_0}{T}\right)^2 + a_3 \left(\frac{T_0}{T}\right)^3, \quad (6)$$

and the constants  $a_i, b_i$  are fixed to reproduce the pure gauge theory thermodynamics with the phase transition at  $T_0 = 270$  MeV. We adopt the values determined in [23] and shown for completeness in Table I. Here  $\phi$  is the gauge-invariant Polyakov loop in the fundamental representation.

Since the Polyakov loop microscopically contains only contribution from the longitudinal gluons while also transverse gluons contribute to the QCD pressure, one could consider more general Wilson lines and also include other loop degrees of freedom, say, adjoint or the sextet. Here we

TABLE I. The parameters used for the effective potential.

<i>LSM:</i>	$v = f_\pi$ 0.093 GeV	$\lambda$ 4.44	$g$ 3.3
<i>NJL:</i>	$m_0$ 5.5 MeV	$\Lambda$ 651 MeV	$G$ 10.08 (GeV) <sup>-2</sup>
<i>Polyakov:</i>	$a_0$ 6.75	$a_1$ -1.95	$a_2$ 2.625
	$a_3$ -7.44	$b_3$ 0.75	$b_4$ 7.5

choose to start with the mean field potential of the fundamental loop parametrized to describe the pure gauge thermodynamics and study how the interactions with the chiral degrees of freedom affect it and compare against full QCD thermodynamics. The extensions towards other possible degrees of freedom we leave for future work. Recently there has been interesting developments in the construction of effective theory for the pure gauge thermodynamics, e.g. [26,27], which could be in principle coupled to chiral fields to obtain an effective theory for QCD. Here we choose to remain with the mean field potential (5) which seems to capture the pure gauge thermodynamics sufficiently well for our purposes.

Then, for a spatially uniform system in thermodynamical equilibrium at temperature  $T$  and quark chemical potential  $\mu$  the partition function is

$$Z = \text{Tr} \exp[-(\mathcal{H} - \mu \mathcal{N})] = \int \mathcal{D}\bar{q} \mathcal{D}q \exp\left[\int_x (\mathcal{L} + \mu \bar{q} \gamma^0 q)\right]. \quad (7)$$

The integration over the spacetime in the action is over the compact Euclidean time direction and over the spatial three-volume  $V$ ,  $\int_x = \int_0^{1/T} d\tau \int_V d^3x$ . Since the action is quadratic in quark fields, the functional integral is easily performed with standard methods, leading to the grand canonical potential

$$\Omega = -\frac{T \ln Z}{V} = U_{\text{chiral}} + U_\phi + \Omega_{\bar{q}q}, \quad (8)$$

where

$$U_{\text{chiral}} = \frac{\lambda^2}{4}(\sigma^2 + \pi^2 - v^2)^2 - H\sigma, \quad \text{LSM} \quad (9)$$

$$U_{\text{chiral}} = \frac{(m_0 - M)^2}{2G}, \quad \text{NJL}$$

for the chiral contribution and  $U_\phi = U(\phi, \phi^*, T)$ . The Wilson line is now  $L = \exp(-A_0/T)$ , and therefore the interactions connecting the deconfinement and chiral sectors become

$$\Omega_{\bar{q}q} = -2N_f T \int \frac{d^3p}{(2\pi)^3} (\text{Tr}_c \ln[1 + L e^{-(E-\mu)/T}]) + \text{Tr}_c \ln[1 + L^\dagger e^{-(E+\mu)/T}] - 6N_f \int \frac{d^3p}{(2\pi)^3} E \theta(\Lambda^2 - |\vec{p}|^2), \quad (10)$$

where the trace over color remains,  $E = \sqrt{\vec{p}^2 + M^2}$  (and further  $M = g\sigma$  in LSM). In LSM we neglect the vacuum contribution term in  $\Omega_{\bar{q}q}$  and in the NJL model it is controlled by the cutoff  $\Lambda$  as indicated in (10). Performing the remaining trace, and using  $\phi = \text{Tr}_c(L)/N_c$  gives

$$\begin{aligned}
& (\text{Tr}_c \ln[1 + L e^{-(E-\mu)/T}] + \text{Tr}_c \ln[1 + L^\dagger e^{-(E+\mu)/T}]) \\
& = \ln(1 + 3(\phi + \phi^* e^{-(E-\mu)/T}) e^{-(E-\mu)/T} + e^{-3(E-\mu)/T}) \\
& \quad + \ln(1 + 3(\phi^* + \phi e^{-(E+\mu)/T}) e^{-(E+\mu)/T} + e^{-3(E+\mu)/T}),
\end{aligned} \tag{11}$$

Note that in principle the chemical potential affects the Polyakov loop potential directly, see [25], but we will not consider these effects. Having determined the grand canonical potential both for the Polyakov loop linear sigma model (PLSM) and Polyakov loop NJL model (PNJL), the thermodynamics is now determined by solving the equations of motion for the mean fields,

$$\frac{\partial \Omega}{\partial \sigma} = 0, \quad \frac{\partial \Omega}{\partial \phi} = 0, \quad \frac{\partial \Omega}{\partial \phi^*} = 0, \tag{12}$$

and then the pressure is given by evaluating the potential on the minimum:  $p = -\Omega(T, \mu)$ . We now proceed to solve numerically the thermodynamics of PLSM and PNJL models and compare them with each other as well as against the numerical results on two-flavor QCD at zero chemical potential.

### III. NUMERICAL RESULTS

#### A. Thermodynamics at $\mu = 0$ , comparison to QCD

Let us first consider the models at zero chemical potential but finite temperature. When finite temperature is considered, it is well known that the quantitative results of chiral effective theories differ: While NJL model predicts chiral restoration at  $T \sim 150$  MeV, the linear sigma model leads to result  $T \sim 190$  MeV [8]; allowing for finite chemical potentials only widens the spread. Including the Polyakov loop has important consequence as now both of these models predict a crossover near  $T \sim 210 \dots 230$  MeV within 20 MeV of each other, as we show in Fig. 1, where we plot the temperature derivatives of the condensates. The location of the peak defines the critical temperature around which the crossover takes place.

Then consider the pressure. The coupled models, PNJL and PLSM, have already been shown to agree with lattice data at and above  $T_c$  fairly well [23,25] with some fine-tuning. Namely, lattice data implies a critical temperature  $T_c \sim 175$  MeV, a value  $\sim 20\%$  lower than we obtain. In [23] it has been noted that better agreement can be achieved in the PNJL model by detuning the Polyakov loop potential away from the pure gauge thermodynamics through shifting of the parameter  $T_0$  down to 190 MeV. Since the lattice data has still some uncertainty to it due to the extrapolation to the continuum limit, we choose not to aim for perfect fits and rather plot the thermodynamical quantities as a function of  $T/T_c$  when comparing different models. Actually, the value of  $T_c$  should be determined by allowing for additional degrees of freedom below  $T_c$  which are not considered in these effective models. We have not included the finite temperature contributions of the pions and more massive resonances, since we do not have a dynamical way to decouple their contribution at high temperatures. However, our aim is to study the interplay of chiral fields and Polyakov loop and the resulting thermodynamics for the temperature range  $T_c < T < 3T_c$  for which the coupled models under consideration are expected work well.

Here, to compare with QCD, we use the numerical result of [16] in which the high-temperature part of the curve is based on the full  $\mathcal{O}(g^6 \log(g))$  calculation in the pure gauge theory, supplemented with a more phenomenological recipe to include the contribution of  $N_f$  massive quarks at order  $\mathcal{O}(g^2)$ . At low temperatures this result is matched smoothly on the resonance gas result from [28]. This QCD + resonance gas result is shown in the left panel of Fig. 2 at  $N_f = 2$  appropriate for this work [29]. Also shown are our results for the pressure obtained from the coupled models PLSM and PNJL as a function of  $t = T/T_c$ . For comparison we show the corresponding results from the LSM and NJL models without the Polyakov loop. Observe how the inclusion of the Polyakov loop increases the result for the absolute value of the pressure by roughly 80%. The addition of the Polyakov loop is therefore necessary in

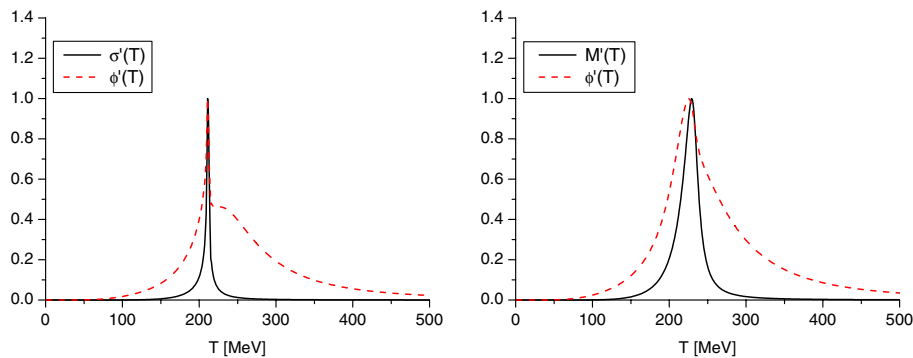


FIG. 1 (color online). Left panel: Temperature derivatives of the mean fields  $\phi(T)$  and  $\sigma(T)$  at  $\mu = 0$  in the PLSM model. Right panel: Same observables as in the left panel but in the PNJL model.

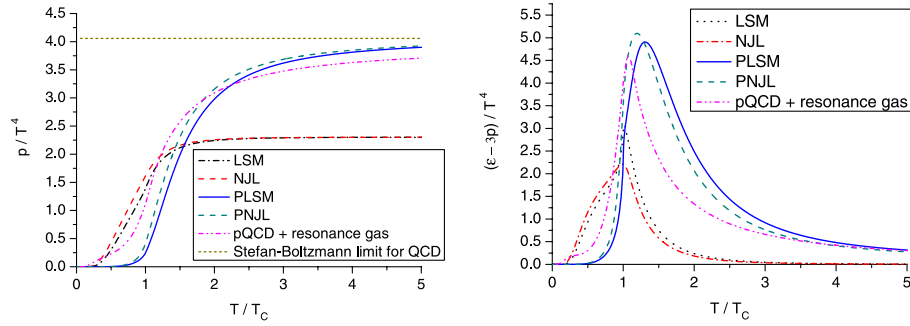


FIG. 2 (color online). Left panel: Pressure from the models with and without the Polyakov loop at  $\mu = 0$ . Also shown is the curve interpolating between the resonance gas and resummed perturbation theory results [16] as well as the constant corresponding to the Stefan–Boltzmann limit of two-flavor QCD. Right panel: Similar figure for the trace anomaly  $(\epsilon - 3P)/T^4$ .

order to quantitatively obtain the required rise in the pressure towards the Stefan–Boltzmann limit of QCD corresponding to the horizontal dashed line in the figure. The difference between the chiral model pressure and the additional increase due to the Polyakov loop can be understood by looking at the contribution of bosons and fermions in the ideal gas result which for zero chemical potentials is

$$p_{\text{SB}} = \frac{\pi^2 T^4}{45} \left( (N_c^2 - 1) + \frac{7N_c N_f}{4} \right).$$

Setting  $N_c = 3$  and  $N_f = 2$ , the ratio of the bosonic and fermionic contributions is  $g_B/g_F = 16/21 \approx 0.76$ .

Both PNJL and PLSM models give a good overall description of QCD pressure above  $T_c$ . They lead to slightly smaller deviation from the ideal gas limit at  $T \sim 4T_c$  than actually observed, but quantitatively this difference is small. Let us then turn to the analysis of more differential observables like the entropy density  $s(T) = p'(T)$ , the energy density  $\epsilon(T) = Ts(T) - p(T)$ , trace of the energy momentum tensor  $\theta_\mu^\mu(T) = \epsilon(T) - 3p(T)$  and the heat capacity  $c(T) = \epsilon'(T) = Tp''(T)$ . These serve as important probes which, together with lattice data, allow us to probe the validity of different models and the knowledge of the temperature dependence of these quantities is important for phenomenology of relativistic heavy ion collisions as well as for cosmology.

Let us first consider the trace of the energy momentum tensor. We show the result of different models in the right panel of Fig. 2. Notice how also here the inclusion of the Polyakov loop is imperative to match lattice data in comparison to LSM and NJL models: First, the addition of the Polyakov loop removes the qualitatively different structures in LSM and NJL model around  $T_c$  and in the coupled models a smooth universal curve results. Second, the inclusion of the Polyakov loop is important also for obtaining agreement with the asymptotic behavior above  $T_c$ . In fact both LSM and NJL models alone predict that at high temperatures  $\theta_\mu^\mu(T) \times T^4 = \text{const}$  contrary to the observation.

The information contained in the trace anomaly can also be represented in terms of the “equation-of-state parameter”  $w(T) = p(T)/\epsilon(T)$  which we show in Fig. 3. Both PLSM and PNJL models give again very similar results, significantly lower than the pQCD result also shown in the figure. The effective model results are similar to recent lattice data [30]. There are two clear features deserving further numerical and theoretical studies: First, the drop near  $T_c$  leads to  $w \sim 0.1$  in PNJL and PLSM models as well as in the lattice data while the perturbation theory result is larger,  $w \sim 0.15$ . Second, below  $T_c$  the pQCD model leads to a larger rise in  $w(T)$  than the lattice data and the PNJL and PLSM models. These features are likely to be affected by the resonance gas dynamics which is now neglected in the effective models but which is present in the pQCD + resonance gas -model.

The information contained in the derivatives defined above can be presented and explored in various ways. We choose to follow the presentation in [16], since that allows also a quantitative comparison against the results from the resummed perturbation theory. In Fig. 4 we plot the effec-

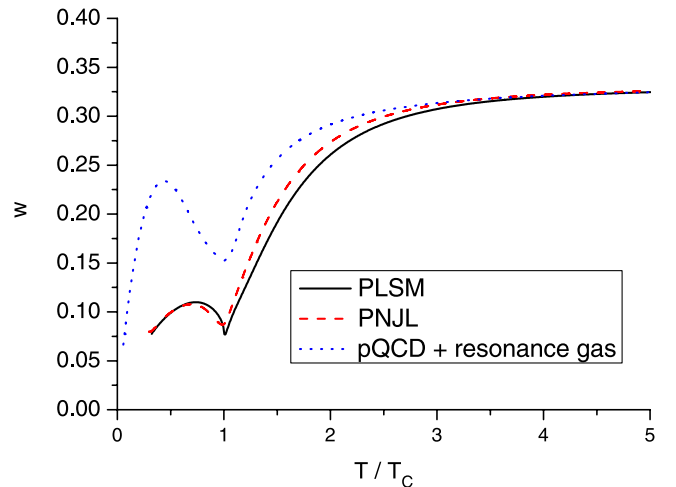


FIG. 3 (color online). The equation-of-state parameter  $w(T) = p(T)/\epsilon(T)$ .

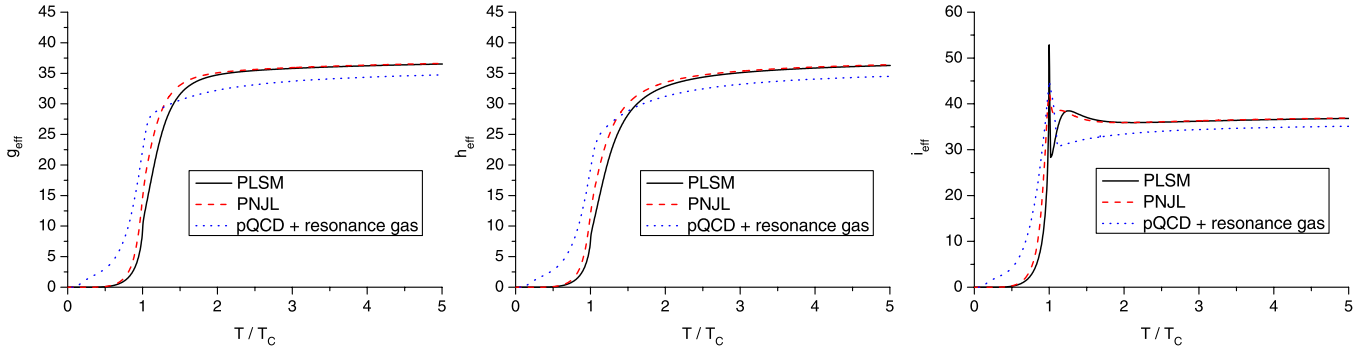


FIG. 4 (color online). Effective degrees of freedom in the PLSM, PNJL and pQCD + resonance gas model [16]. Left panel:  $g_{\text{eff}}(T)$  at  $\mu = 0$ . Middle panel:  $h_{\text{eff}}(T)$  at  $\mu = 0$ . Right panel:  $i_{\text{eff}}(T)$  at  $\mu = 0$ .

tive numbers of degrees of freedom defined by

$$g_{\text{eff}} \equiv \frac{\epsilon(T)}{\left[\frac{\pi^2 T^4}{30}\right]}, \quad h_{\text{eff}} \equiv \frac{s(T)}{\left[\frac{2\pi^2 T^3}{45}\right]}, \quad i_{\text{eff}} \equiv \frac{c(T)}{\left[\frac{2\pi^2 T^3}{15}\right]}. \quad (13)$$

Looking at the effective degrees of freedom, we again see that both PLSM and PNJL model results are consistent with each other and with the corresponding QCD + resonance gas results. Only  $i_{\text{eff}}$  shows some qualitative differences in how these two models respond to finite temperature as the peak at  $T_c$  is sharper in PLSM model than in PNJL model. This peak arises since  $i_{\text{eff}}$  is proportional to heat capacity which diverges in a second order phase transition. Another issue present in the temperature dependence of  $i_{\text{eff}}$  is a small second peak visible very weakly in PNJL model but more strongly in PLSM model. This is due to the remnant of the deconfinement transition described by the temperature dependence of the parameters in the Polyakov loop potential. Note how it is vital to look at more differential observables, second derivatives in this case, to see this effect. More precise lattice data is needed to determine whether the central assumption of these models about two independent phase transitions connected by interactions is indeed correct.

## B. Thermodynamics at $\mu \neq 0$ : Location of the critical point?

Let us then consider the consequences of nonzero net-quark density by allowing for a finite chemical potential. As a starting point we will use the grand canonical potential derived in Sec. II, and neglect a possible explicit  $\mu$ -dependence of the Polyakov loop potential which has been discussed e.g. in Ref. [25].

First we study whether the coincidence of deconfinement and chiral symmetry restoration holds also at finite chemical potential. In Fig. 5 we show the derivatives of the condensates as a function of temperature at  $\mu = 100$  MeV and in Fig. 6 at  $\mu = 250$  MeV. We observe a coincident peaks in the derivatives of the condensates in both of these effective models. Note that at finite chemical potential  $\phi$  and  $\phi^*$  are no more equal and note also that at large chemical potentials already at first derivatives of the condensates a double peak structure arises. The latter is due to the fact that as chemical potential is increased, the critical temperature in the chiral sector decreases as shown by the location of the left-most peak in the figures, while the remnant of the deconfinement transition in the Polyakov loop potential is unaffected by the value of the chemical potential and remains visible at temperature  $T \sim 200$  MeV. Of course the meaning of the peaks in  $\phi$  (and

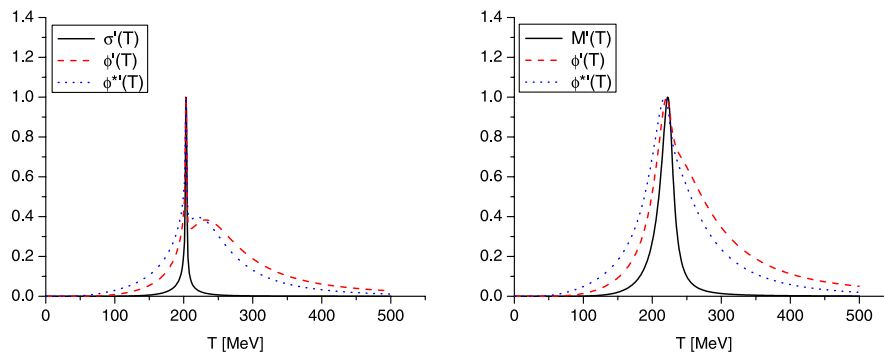


FIG. 5 (color online). Temperature derivatives of the mean fields  $\phi(T)$  and  $\sigma(T)$  at  $\mu = 100$  MeV. Left panel: The PLSM model. Right panel: The PNJL model.

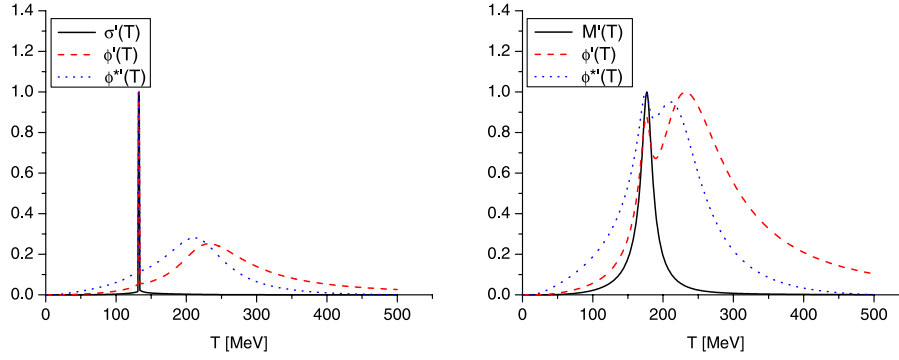


FIG. 6 (color online). Temperature derivatives of the mean fields  $\phi(T)$  and  $\sigma(T)$  at  $\mu = 250$  MeV. Left panel: The PLSM model. Right panel: The PNJL model.

$\phi^*$ ) and their relation to deconfinement is debatable; perhaps the system becomes deconfined at temperature related to the second peak in  $\phi$ . This interpretation can be motivated by studying the value of the Polyakov loop which is small at temperatures near the peak in the chiral condensate and of the order of 0.5 at higher temperatures around the second peak. In any case, as the two distinct transitions underlying these effective models are separated over a wider temperature range, their separate features become also more visible. Hence, this provides another way to numerically investigate the correctness of the initial assumption of independent deconfinement and chiral symmetry restoration underlying these models.

Next, we will use the information in the temperature dependence of the condensates to obtain  $(T, \mu)$ -phase diagrams of these models. As already discussed above, in these models the expectation value of the Polyakov loop varies rapidly first when the chiral condensate  $\sigma$  drops as chiral symmetry is restored and second, at higher temperature due to the temperature dependent coefficient  $b_2(T)$  in the Polyakov loop potential. Moreover, at high temperature the temperature derivatives of the expectation values of Polyakov loop  $\phi$  and its conjugate  $\phi^*$  display noncoincident peaks. The whole situation is summarized for PLSM in Fig. 7, where we have plotted in the  $(T, \mu)$ -plane the locations where the coincident peaks in the temperature derivatives of  $\phi$ ,  $\phi^*$  and  $\sigma$  as well as the second peaks in  $\phi$  and  $\phi^*$  are shown. Note that in the LSM model the double peak structure in  $\phi$  remains visible also at  $\mu = 0$ . This double peak structure is a feature of these effective models, and whether true in real QCD remains to be determined. In what follows, we therefore choose to plot the phase diagrams showing only the location of the coincident peaks of  $\phi$ ,  $\phi^*$  and  $\sigma$  corresponding to a chiral phase transition. See also [31]. We show the  $(T, \mu)$  phase diagram in Fig. 8, where two sets of curves are plotted. These two sets correspond to the two chiral models with and without the Polyakov loop. The solid lines correspond to the first order transition and the dotted lines to the crossover. The lines have been determined by finding the location of the peak in

the chiral condensate  $\sigma(T)$  at each chemical potential. The phase at low temperature and low net-quark density is confined and chiral symmetry is broken, while at high temperature the chiral symmetry is restored and the system is deconfined. The two models yield very different values for the location of the critical point: while the PLSM gives  $(T_c, \mu_c) = (195, 141)$  for the position of the critical point, the PNJL model yields  $(88, 329)$ . This can be due to several reasons, e.g. the neglect of the possible chemical potential dependence of the Polyakov loop potential. On the other hand, this can be due to the neglect of possible relevant degrees of freedom. It is likely that at finite chemical potential diquark degrees of freedom become important and should be taken into account; see [32]. This situation would be similar to the differences between LSM and NJL models at finite temperature which were shown to reduce once the Polyakov loop dynamics is accounted for.

To discover the critical point experimentally in heavy ion collisions, it would be desirable to have a reliable quantitative theoretical estimate of its location. As we have explicitly seen here, various effective theory esti-

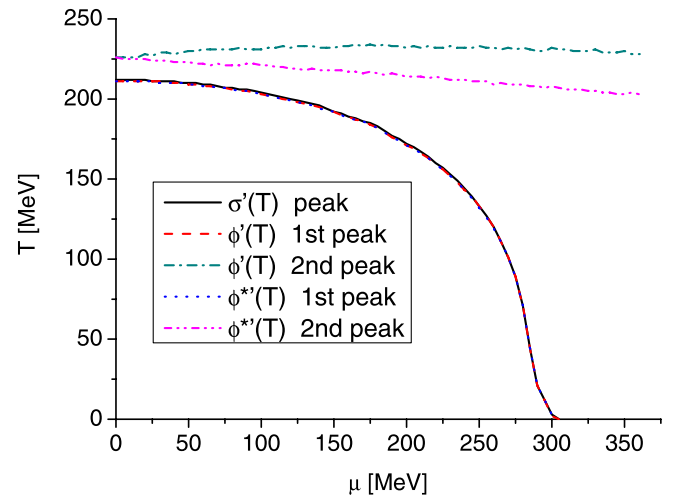


FIG. 7 (color online). Location of the peaks in the temperature derivatives of  $\sigma$ ,  $\phi$  and  $\phi^*$  over the  $(T, \mu)$ -plane.

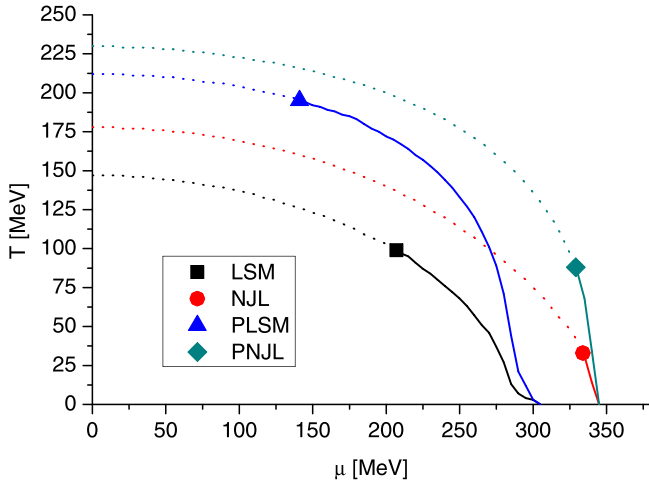


FIG. 8 (color online). The  $(T, \mu)$  phase diagram. Left-most pair of curves shows the result for the LSM and PLSM while the second pair is for the NJL and PNJL models. The solid part of the curve denotes a first order transition while the dashed part is a crossover.

mates deviate a lot when finite chemical potentials are considered. The lattice determinations using different techniques also lead to very different results for the location of the critical point. For example, for two flavors the authors of [12] find the critical point at  $\mu_B \sim 360$  MeV while in [13] a value  $\mu_B \sim 180$  MeV is reported. Currently the existence of the critical point is debatable [14,15], and in any case one should be careful in drawing any conclusions from  $N_f = 2$  results to the physical  $2 + 1$  case.

With these remarks in mind, let us assume that the critical point in the  $(T, \mu)$  plane exists as implied by the PNJL and PLSM models. Then, even if the exact location of the critical point is not known, one may argue in favor of its experimental detection if the spacetime evolution of the strongly interacting elementary particle matter is such that the system passes through the vicinity of the critical point starting from almost any initial condition. The outcomes of such *focusing* behavior have been recently advocated for in [33] strongly motivated by [34]. However, the focusing

observed in [34] can be due to the particular equation of state applied in that work and is not a general feature of hydrodynamics approach applied successfully to describe the RHIC data as in e.g. [35]. Given the success of ideal fluid hydrodynamics in the description of the RHIC data, it is likely that the system expands nearly isentropically. Therefore, to decide whether the focusing behavior in the models studied here should occur, we find the adiabats of PLSM and PNJL models in the  $(T, \mu)$  plane. The result is shown in Figs. 9 and 10, and the conclusion for both of these models is that no strong focusing behavior exists. Based on these figures we conclude that for the hydrodynamical evolution starting from a near-zero net-quark density, as would be the case in a central Au + Au collision at RHIC, the trajectory of the system in  $(T, \mu)$ -plane is nonfocusing. As the closeups in the right panels of Figs. 9 and 10 show, there is no special behavior near the critical points. This result is similar to the one obtained on the lattice [30].

Note that from the behavior of the isentropic lines one can deduce the location of the phase boundary exactly where the coincident peaks in the temperature derivatives of  $\sigma$  and  $\phi$  would put it. These lines show no special behavior when crossing the lines indicating the location of the second peaks in the temperature derivatives of  $\phi$  and  $\phi^*$ .

Another interesting quantity is the sound speed  $c_s(T) = \sqrt{\partial \epsilon / \partial p}$  shown in Fig. 11 for chemical potentials near the critical one. The stronger dependence of the location of the minimum in  $c_s(T)$  as a function of the chemical potential in PNJL model is due to the fact that near the critical point the value of  $T_c(\mu)$  changes more rapidly than in the case of PLSM model. Together with Figs. 9 and 10 we see from here that in the hydrodynamical evolution the sound speed is very small during the part of the evolution the system spends near the phase transition region. At the  $(T, \mu)$  regions relevant for RHIC and LHC/ALICE phenomenology, the sound speed is probably well approximated by the  $\mu = 0$  result as the system evolves very close to the  $\mu \sim 0$  axis along a nearly parallel trajectory until low temperatures deep in the hadronic phase are reached and the

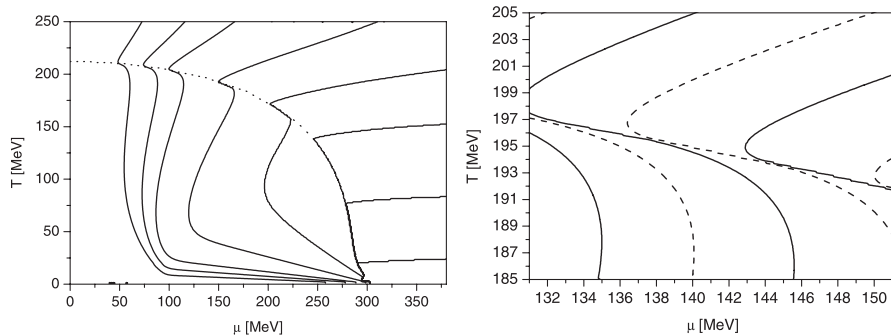


FIG. 9. Left panel: Constant  $S/N$  curves in the PLSM model. Right panel: A close-up on the critical point at  $(T_c, \mu_c) = (195, 141)$  MeV. Every second curve has been drawn with the dashed line to enhance readability.

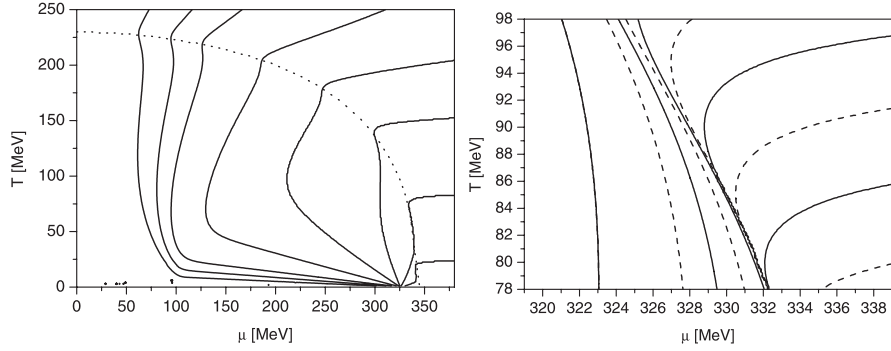


FIG. 10. Left panel: Constant  $S/N$  curves in the PNJL model. Right panel: A close-up on the critical point at  $(T_c, \mu_c) = (88, 329)$  MeV.

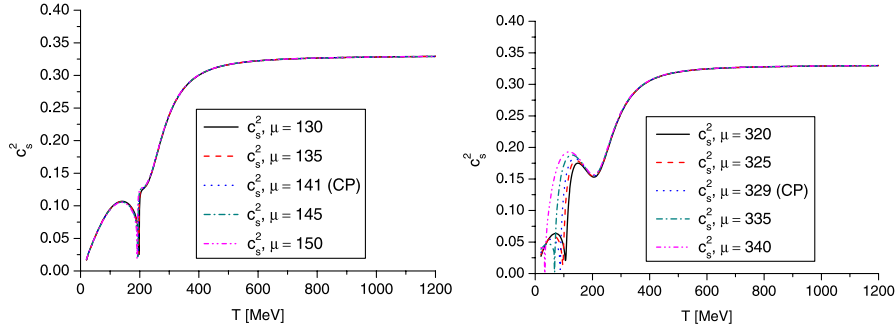


FIG. 11 (color online). Left panel: Sound speed at different chemical potentials in the PLSM model. Right panel: Same for the PNJL model.

trajectory bends to end at the finite value  $\mu_{\text{vac}}$  at zero temperature. However, if it was possible to create systems which would follow the trajectory bending along the phase boundary as the ones at large chemical potential in Figs. 9 and 10, then the sound speed could stay small over larger temperature range and this might have consequences for e.g. Mach cones created by high momentum jets traversing the thermal medium [36]. On the other hand, while the collisions planned at the GSI/FAIR facility might lead to more optimal  $S/N$  trajectories for this argument to work, the probability for the production of the required high momentum probes is much smaller. However, we remind the reader that a thorough investigation of the heavy ion phenomenology should be carried out with an effective theory suited to describe the  $N_f = 2 + 1$  case.

#### IV. CONCLUSIONS AND OUTLOOK

In this paper we have analyzed thermodynamics of two effective theories for QCD which contain as relevant degrees of freedom the Polyakov loop and chiral fields within a framework proposed to correctly interpolate between the pure gauge, center symmetric, and chirally symmetric two-flavor QCD. At zero chemical potential but finite temperature we observed that the contribution from the Polyakov loop to thermodynamical quantities like the pressure is

very important; roughly half of the total pressure. Another aspect which underlines the importance of the Polyakov loop sector is the fact that adding it to the dynamics tends to diminish the qualitative differences present in the bare chiral theories at finite temperature. We have considered explicitly two realizations, the linear sigma model and the NJL model. Our results indicate that even if both models describe the chiral dynamics of the QCD vacuum correctly, they must be supplied by other degrees of freedom in order to obtain quantitatively correct effective description of QCD thermodynamics. We presented a comparison with a recent result which interpolates between resummed perturbation theory result and resonance gas result [16], and outlined how future lattice simulations could allow one to obtain more insight into the QCD dynamics near the phase transition.

We also considered finite chemical potentials and determined the  $(T, \mu)$  phase diagram of these theories. Here we observed large discrepancies between the PLSM and PNJL models. Based on the above discussion, an obvious explanation would be that some important dynamics is again being missed. A natural candidate for a new relevant degree of freedom is the diquark condensate responsible for the color superconducting phenomena. We aim to extend our work towards this direction next. We also determined the lines of constant  $S/A$  in the  $(T, \mu)$ -plane and

discussed the implications for the equation of state as well as for the possible focusing behavior relevant for the experimental discovery of the QCD critical point.

These results can be used for phenomenological applications. The parametrization of the equation of state obtained from these models has been shown to agree with lattice data at  $\mu = 0$  but is easily evaluated also at finite values of the chemical potential. Hence it could be applied in hydrodynamical simulations of ultrarelativistic heavy ion collisions. We have evaluated the sound speed, and shown that on the hydrodynamically relevant trajectories there may be substantial temperature range over which the sound speed is small. However, it may prove difficult in the laboratory to create systems which would follow these particular trajectories. We hope to extend these phenomenological studies within realistic hydrodynamics in near future.

There are several improvements to be addressed. We have already stressed that below the critical temperature, a more careful treatment of hadronic degrees of freedom is required, and the lack of this treatment is best seen in the apparent underestimate of the pressure below  $T_c$ . Another

issue clearly concerns the number of active flavors. Here we have concentrated only on the case of two flavors, while for more quantitative phenomenology it is vital to have the effects of the strange quark under control. However, as a first approximation for the equation of state at small chemical potential it should be reasonable to multiply the pressure by the overall factor  $g_{\text{SB}}(N_f = 3)/g_{\text{SB}}(N_f = 2)$  where  $g$  counts both the bosonic and fermionic degrees of freedom. Lattice data [37] indicates that the flavor dependence of the QCD pressure is dominated by the Stefan-Boltzman factor and the above scaling can be applied within 10% accuracy. Similar reasoning has been used also in [16] to obtain the perturbative QCD result for full  $N_f$  flavors with masses  $\{m_{N_f}\}$ . We aim to address these issues in future work within the effective theory framework discussed here.

### ACKNOWLEDGMENTS

We thank A. Dumitru and T. Renk for useful discussions and K. J. Eskola for careful reading of the manuscript. T. K. thanks the Väisälä foundation for financial support.

- 
- [1] B. Svetitsky and L.G. Yaffe, Nucl. Phys. **B210**, 423 (1982).
  - [2] A. M. Polyakov, Phys. Lett. **72B**, 477 (1978); G. 't Hooft, Nucl. Phys. **B138**, 1 (1978).
  - [3] P.H. Damgaard, Phys. Lett. **B 194**, 107 (1987); J. Engels *et al.*, Z. Phys. C **42**, 341 (1989); J. Engels *et al.*, Phys. Lett. **B 365**, 219 (1996).
  - [4] P. Bacilieri *et al.*, Phys. Rev. Lett. **61**, 1545 (1988); F.R. Brown *et al.*, Phys. Rev. Lett. **61**, 2058 (1988).
  - [5] O. Kaczmarek *et al.*, Phys. Rev. D **62**, 034021 (2000).
  - [6] G.G. Batrouni and B. Svetitsky, Phys. Rev. Lett. **52**, 2205 (1984); A. Gocksch and M. Okawa, Phys. Rev. Lett. **52**, 1751 (1984); F. Green and F. Karsch, Phys. Rev. D **29**, 2986 (1984); J.F. Wheeler and M. Gross, Phys. Lett. **144B**, 409 (1984).
  - [7] F. Wilczek, Int. J. Mod. Phys. A **7**, 3911 (1992); **7**, 6951 (1992).
  - [8] O. Scavenius, A. Mocsy, I.N. Mishustin, and D.H. Rischke, Phys. Rev. C **64**, 045202 (2001).
  - [9] S. Holtmann and T. Schulze, Phys. Rev. E **68**, 036111 (2003).
  - [10] R.D. Pisarski and D.H. Rischke, Phys. Rev. D **61**, 051501 (2000); D.K. Hong, Phys. Lett. **B 473**, 118 (2000); P.T. Reuter, Q. Wang, and D.H. Rischke, Phys. Rev. D **70**, 114029 (2004); **71**, 099901(E) (2005).
  - [11] Z. Fodor, S. D. Katz, and K. K. Szabo, Phys. Lett. **B 568**, 73 (2003); C.R. Allton *et al.*, Phys. Rev. D **66**, 074507 (2002); P. de Forcrand and O. Philipsen, Nucl. Phys. **B673**, 170 (2003); M. D'Elia and M. P. Lombardo, Phys. Rev. D **67**, 014505 (2003).
  - [12] Z. Fodor and S.D. Katz, J. High Energy Phys. **04** (2004) 050.
  - [13] R.V. Gavai and S. Gupta, Phys. Rev. D **71**, 114014 (2005).
  - [14] O. Philipsen, arXiv:0710.1217.
  - [15] P. de Forcrand, S. Kim, and O. Philipsen, Proc. Sci. LAT2007 (2007) 178 [arXiv:0711.0262].
  - [16] M. Laine and Y. Schroder, Phys. Rev. D **73**, 085009 (2006).
  - [17] A. Tawfik, Phys. Rev. D **71**, 054502 (2005); F. Karsch, K. Redlich, and A. Tawfik, Eur. Phys. J. C **29**, 549 (2003).
  - [18] F. Karsch and M. Lutgemeier, Nucl. Phys. **B550**, 449 (1999).
  - [19] G.E. Brown, A.D. Jackson, H.A. Bethe, and P.M. Pizzochero, Nucl. Phys. **A560**, 1035 (1993); S. Dikal, E. Laermann, and H. Satz, Nucl. Phys. **A702**, 159 (2002); Y. Hatta and K. Fukushima, Phys. Rev. D **69**, 097502 (2004).
  - [20] A. Mocsy, F. Sannino, and K. Tuominen, Phys. Rev. Lett. **91**, 092004 (2003); A. Mocsy, F. Sannino, and K. Tuominen, J. High Energy Phys. **03** (2004) 044; A. Mocsy, F. Sannino, and K. Tuominen, Phys. Rev. Lett. **92**, 182302 (2004).
  - [21] F. Sannino and K. Tuominen, Phys. Rev. D **70**, 034019 (2004).
  - [22] K. Fukushima, Phys. Lett. **B 591**, 277 (2004).
  - [23] C. Ratti, M. A. Thaler, and W. Weise, Phys. Rev. D **73**, 014019 (2006).
  - [24] P. Costa, M. C. Ruivo, and C. A. de Sousa, Phys. Rev. D **77**, 096001 (2008); P. Costa, C. A. de Sousa, M. C. Ruivo, and H. Hansen, arXiv:0801.3616.
  - [25] B.J. Schaefer, J.M. Pawłowski, and J. Wambach, Phys. Rev. D **76**, 074023 (2007).

- [26] A. Vuorinen and L.G. Yaffe, Phys. Rev. D **74**, 025011 (2006); Ph. de Forcrand, A. Kurkela, and A. Vuorinen, arXiv:0801.1566.
- [27] R.D. Pisarski, Phys. Rev. D **74**, 121703 (2006).
- [28] F. Karsch, K. Redlich, and A. Tawfik, Phys. Lett. B **571**, 67 (2003).
- [29] We thank M. Laine for providing the numerical results of [16] for the  $N_f = 2$  case.
- [30] S. Ejiri, F. Karsch, E. Laermann, and C. Schmidt, Phys. Rev. D **73**, 054506 (2006).
- [31] C. Sasaki, B. Friman, and K. Redlich, Phys. Rev. D **75**, 074013 (2007).
- [32] S. Roessner, C. Ratti, and W. Weise, Phys. Rev. D **75**, 034007 (2007).
- [33] R. A. Lacey *et al.*, Phys. Rev. Lett. **98**, 092301 (2007).
- [34] C. Nonaka and M. Asakawa, Phys. Rev. C **71**, 044904 (2005).
- [35] K.J. Eskola, H. Honkanen, H. Niemi, P.V. Ruuskanen, and S.S. Rasanen, Phys. Rev. C **72**, 044904 (2005).
- [36] T. Renk and J. Ruppert, Phys. Rev. C **72**, 044901 (2005).
- [37] F. Karsch, E. Laermann, and A. Peikert, Phys. Lett. B **478**, 447 (2000).